NATIONAL TECHNICAL UNIVERSITY OF UKRAINE

“IGOR SIKORSKY KYIV POLYTECHNIC INSTITUTE”

Faculty of Instrumentation Engineering

Department of Automation and Non-Destructive Testing Systems

Approved for defense:

Acting Head of Department

Halyna BOHDAN

“____” ________ 20__

Diploma Project

for the degree of Bachelor

in the educational-professional program

“Computer-Integrated Systems and Technologies in Instrument Making”

specialty 151 “Automation and Computer-Integrated Technologies”

Thesis Title: “Quadrotor UAV Attitude Estimation System”

Performed by:
4th-year student, Group PK-11
Ivanna Dovbysh

Supervisor:
Assosiate Professor, PhD
Oleksandr Muraviov

Reviewer:
Assosiate Professor, PhD
Oleg Kozyr

I certify that this project contains no plagiarism from other sources without appropriate references.
Student’s signature: ____________

Kyiv – 2025

Diploma Project Documentation List

№	Format	Code	Title	Pages	Notes
1	A4		Assignment for Bachelor's Project	2	
2	A4	PK11.040000.000 EN	Explanatory Note	64	
3	A2	PK11.040000.000 SD	Structural Diagram	1	
4	A2	PK11.040000.000 FD	Functional Diagram	1	
5	A2	PK11.040000.000 ES	Electrical Schematic Diagram	1	
6	A2	PK11.040000.000 OA	Operation Algorithm	1	
7	A1	PK11.040000.000 AD	Assembly Drawing	1	

	Name	Signature	Date	PK11.040000.000		
Developer	Dovbysh I.O.			Diploma Project Documentation List	Лист	Листів
Supervisor	Muraviov O.V.				1	1
Consultant					Igor Sikorsky KPI Dept. ASNC Group PK-11	
N/contr.						
Head of dept.						

Explanatory Note

to the Diploma Project

on the topic: “Quadrotor UAV Attitude Estimation System”

Kyiv – 2025

NATIONAL TECHNICAL UNIVERSITY OF UKRAINE
"IGOR SIKORSKY KYIV POLYTECHNIC INSTITUTE"

Faculty of Instrument Engineering

Department of Automation and Non-Destructive Control Systems

Level of higher education – First (Bachelor's)

Specialty – 151 "Automation and Computer-Integrated Technologies"

Educational and professional program: "Computer-Integrated Systems and Technologies in Instrument Making"

APPROVED

Acting Head of Department

Halyna BOHDAN

"____" ________ 20__

ASSIGNMENT
for the Diploma project of the student
Ivanna Dovbysh

1. Project Title: "Quadrotor UAV Attitude Estimation System", supervisor: Oleksandr Muraviov, associate Professor, PhD, approved by university order dated "26" May, 2025 № 1765-c

2. Project submission deadline: 9th of June 2025.

3. Initial data for the project:Develop a quadrotor drone, which is able to work in both indoor and outdoor environments, autonomously estimating the position and orientation in relativeness with the initial state. The drone has to be able to transform the high level commands ”take off”, ”move forward”, ”move backward”, ”move to the right”, ”move to the left”, ”rotate left” and ”rotate

right" to the low level commands for the motors. The desired radius for drone operation is 5 m, the weight of the drone should not exceed 500 g.

4. Contents of the explanatory note: Chapter 1. Literature Overview; Chapter 2. Design of a UAV Attitude Estimation System; Chapter 3. Development of UAV Architecture for Attitude Estimation; Chapter 4. Software development for the UAV attitude estimation system.

5. List of graphic materials (including required drawings, posters, presentations, etc.): structural diagram, functional diagram, electrical schematic diagram, operation algorithm, assembly drawing, 2 posters, project presentation.

7. Date of assignment issuance: 17th March 2025.

Project Timeline (Schedule)

№	Stage of project development	Deadline	Note
1	Literature review	21.03.2025	
2	Structural diagram design	28.03.2025	
3	Mathematical model creation	11.04.2025	
4	Functional diagram design	18.04.2025	
5	Component selection	2.05.2025	
6	Electrical schematic diagram design	9.05.2025	
7	Algorithm development	23.05.2025	
8	Assembly drawing creation	30.05.2025	
8	Formatting the diploma project	8.06.2025	

Student: Ivanna DOVBYSH

Supervisor: Oleksandr MURAVIOV

АНОТАЦІЯ

Головним завданням даного дипломного проєкту є розробка системи визначення орієнтації та позиції, яка дозволяє дрону самостійно виконувати завдання високого рівня, такі як «злетіти» або «рухатися вперед». Цей проєкт є підґрунтям для подальших досліджень в області автономності БПЛА.

В рамках проєкту була розроблена інерціальна система навігації, яка дозволяє дрону працювати у відомому середовищі, визначаючи положення відносно початкової позиції. Проаналізовано алгоритми обробки даних, що забезпечують високу точність вимірювань. В даному випадку, розширений фільтр Калмана виконує роль локального фільтра, який прибирає шум і випадкові величини у вимірюваннях і застосовується для вихідних даних кожного датчика. Комплементарний фільтр об’єднує дані з різних джерел, що мінімізує дрейф у часі.

В якості супровідної документації, що ілюструє розроблену систему, створено структурну, функціональну та електричну принципову схеми.

Ключові слова: безпілотний літальний апарат, визначення орієнтації, інерціальна система навігації, позиція, орієнтація, фільтрація даних, об’єднання датчиків, керування БПЛА.

ABSTRACT

The main target of this diploma project is to develop an attitude estimation system, which allows the drone to perform high-level tasks, such as ”take off” or ”move forward” independently. This project is a convenient ground for further research in the field of the UAV autonomy.

Within the framework of this project the inertial navigation system was developed, what allows drone to operate in known environment, estimating the pose with respect to the initial position. Data processing algorithms are analyzed, to provide high accuracy of the measurements. Extended Kalman filter serves as a local observer, that canceling noise and random values and applied to the output of each sensor and the complimentary filter fuses data from different sources to minimize drift in time.

As a supporting documentation, that illustrates the developed algorithms, structural, functional and electrical schematic diagram were created.

Key words: unmanned aerial vehicle, attitude estimation, inertial navigation system, position, orientation, data filtering, sensor fusion, UAV control.

ACRONYMS

AI artificial intelligence.

DC direct current.

GNSS global navigation satellite system.

GPS global positioning system.

IMU inertial measurement unit.

INS inertial navigation system.

SLAM simultaneous localization and mapping.

UAV unmanned aerial vehicle.

VIO visual inertial odometry.

VTOL vertical take off and landing.

CONTENTS

INTRODUCTION

Unmanned aerial vehicles (UAVs) are increasingly being used in a wide variety of areas, from military and civilian intelligence to environmental monitoring, agriculture, logistics, and rescue operations. They can save lives by replacing humans with drones in dangerous environments or by making rapid deliveries of critical medicines. UAVs increase the efficiency of agriculture by continuously monitoring, inspecting, and cultivating land. UAVs play an important role in achieving the Global Sustainable Development Goals, such as ending hunger, good health, combating climate change, and sustainable cities and communities. Therefore, improving the efficiency of drones will not only contribute to the development of science and technology, but also improve the life of society.

The main direction of UAV development is to increase the level of their autonomy, which will allow them to analyze the environment, navigate in space and make decisions on their own. The first task when implementing autonomy is to allow the drone to understand where it is and in what position. To do this, each drone is equipped with an orientation system that allows it to determine its location relative to the environment or relative to the starting point of flight - in particular, to determine the tilt angles, direction of movement, height, coordinates, and other spatial characteristics. The orientation system affects further control algorithms.

Orientation system reduces the requirements for UAV pilot qualifications, and sometimes completely eliminates the need for constant human control.

CHAPTER 1. LITERATURE REVIEW

1.1 Types of Multirotor UAVs

UAVs are becoming an inseparable part of infrastructure, farming, media, rescue operations, and research due to the number of processes they allow us to automate and simplify. As the difficulty of tasks increases, new forms of drones emerge. The most popular are multi-rotor, fixed-wing, and single-rotor drones (Figure 1.1). With the aim of combining advantages of different types, hybrid UAVs are produced [1, 2].

These hybrid platforms seek to merge the vertical take-off and landing (VTOL) capability of multi-rotors with the endurance and speed of fixed-wing systems, making them suitable for long-range missions in constrained or dynamic environments. As the field advances, UAV design increasingly reflects the specific needs of the application—whether it is precision agriculture, persistent surveillance, or autonomous exploration—driving innovation in airframe configurations, energy efficiency, and onboard decision-making systems.

(a) (b) (c)

Figure 1.1. Types of UAVs: (a) multi-rotor drone [3]; (b) fixed-wing drone [4]; (c) single-rotor drone [5].

Due to their range of advantages, multi-rotor UAVs remain the most common. To begin with, they are easy to use and operate. These drones can take various forms and sizes, making them highly adaptable to specific tasks. Moreover, by changing the number of rotors, the total thrust can be increased, which allows for extended payload capacity. Multi-rotor drones show great performance in tasks where hover flight is required: fire extinguishing, farming, video recording, following animals or people, landscape scanning, and monitoring.

Their ability to maintain stable flight in place enables precise positioning and maneuvering in cluttered or unpredictable environments. This makes them especially useful in urban areas, indoors, or during search-and-rescue missions where agility and control are critical. In addition, the relative simplicity of their mechanical design facilitates rapid prototyping and modification, which accelerates their adoption in research and development. However, their limited flight time and range, due to high energy consumption during hover, remain ongoing challenges, often addressed through improvements in battery technology or the use of tethered power systems.

1.1.1 Classification of the Multirotor UAVs

"Multi-rotor" stands for drones, that have more than one rotor. Usually, this number varies from 2 to 8. And the names of the drones are given accordingly (Figure 1.2).

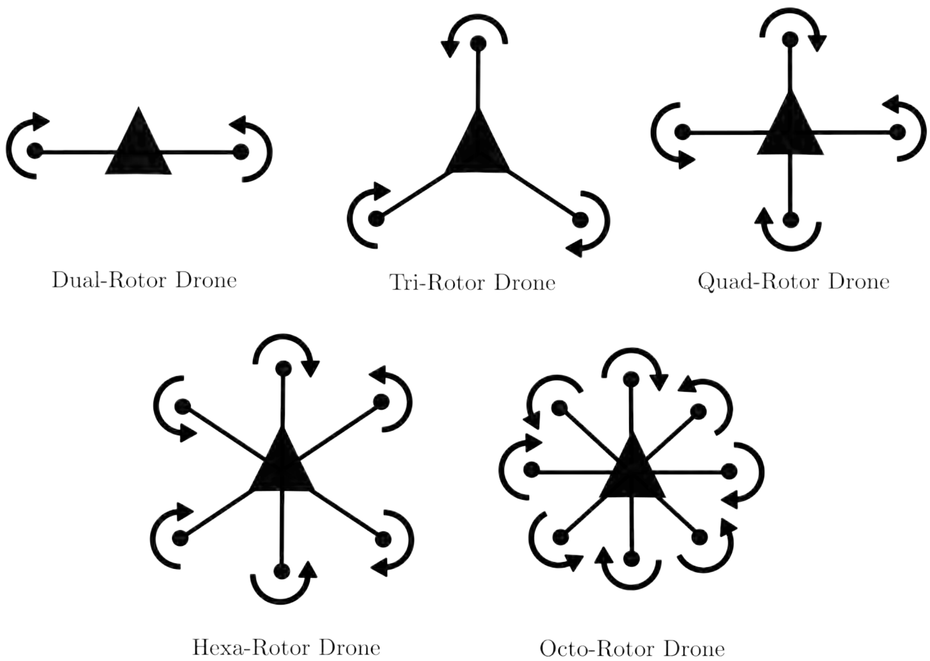

Figure 1.2. Configurations of multirotor UAVs

The number of rotors affects the thrust and control-allocation matrix M, which will be further discussed in section 2.7 [6].

Among multi-rotor UAVs the quadrotors remain the most popular because of their simple mechanical design, stability and cost-effectiveness. However, they can also be divided to different configurations, as it is shown on Figure 1.3. The two most common arrangements are the '+' and 'x' configurations.

In quadrotor usually two motors are rotating clockwise, and two counter clockwise, what allows to reduce the undesirable torque [1]. The selection of pairs that are moving in one direction should be considered, while working on UAV dynamics, as it will change the control-allocation matrix M [6].

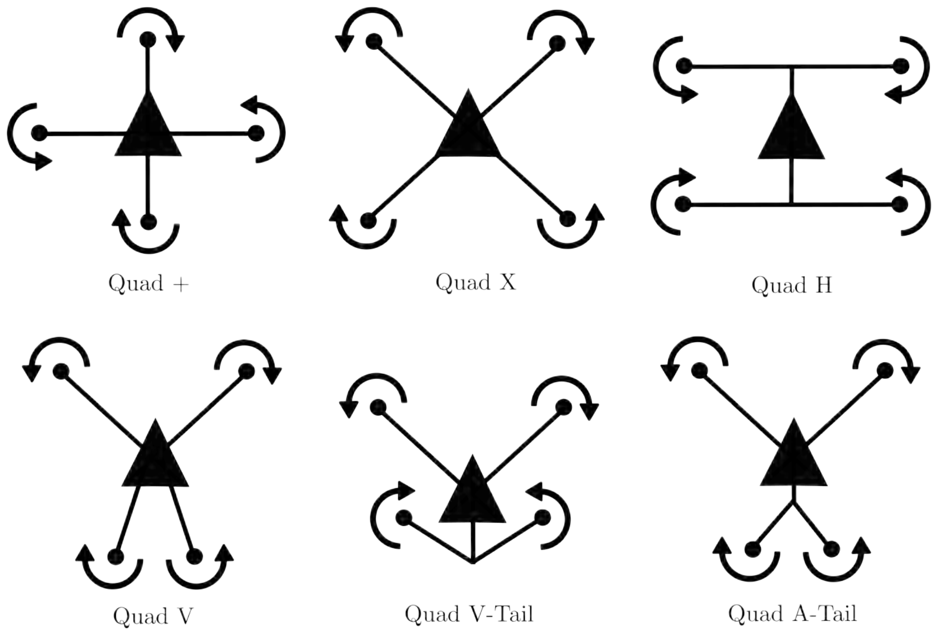

Figure 1.3. Configurations of quad-rotor UAVs

This matrix defines how individual rotor thrusts contribute to the total force and moments acting on the UAV, and is essential for generating accurate attitude and thrust commands. Any change in the rotor configuration—such as altering motor order, direction of rotation, or arm symmetry—modifies M, potentially requiring updates to the control laws or gains used in the flight controller. The estimation algorithm will be further discussed in section 2.5.

1.1.2 Classification of the UAVs According to Their Mass

Another important classification of UAVs is their division according to their mass [7]. The summary of classification and possible applications for each type is demonstrated in Table 1.1. Possible payload, maximum flight time and mission radius is increasing with the drone‘s size. These characteristics might not influence the estimation algorithms, but they define the possible navigation systems that might be installed onboard. Moreover, larger possible payload increases the onboard computation power, which enables implementing complex nonlinear observers and artificial intelligence (AI) technologies [8, 9].

Table 1.1. UAV classification based on weight

Category	Mass (kg)	Payload (kg)	Possible applications
Micro	<2	<1	Indoor inspection, swarm robotics research, education, hobby flying, short-range environmental sensing.
Mini	2 - 25	2 - 8	Precision agriculture (e.g. crop health monitoring), infrastructure inspection, aerial photography, security patrols, disaster response mapping.
Small	25 - 100	4 - 12	Search and rescue in rough terrain, LiDAR mapping, logistics (e.g. medical supply delivery), coastal surveillance.
Medium	150 - 600	8 - 20	Border surveillance, environmental monitoring (e.g. marine pollution), pipeline inspection, cargo transport in remote areas.
Large	>600	>20	Military reconnaissance, long-endurance cargo delivery, high-altitude weather observation, wide-area surveillance.

1.2 Navigation of UAVs

Precise navigation - is the main task for any autonomous vehicle. To solve this issue vehicle or robot needs to understand its position with relativeness to environment (localization), by using the pre-existed map or creating the new one by exploring surroundings. The localization requires the estimation of both position and orientation. Moreover, vehicles must to build the optimal path in the environment (either known or explored) to perform different tasks.

Navigation gets more complicated when the environment is partially known, unobservable or dynamic. The majority of existing frameworks do not show acceptable results in cases of unpredictable challenges, as they are not combining conflict avoidance, environmental sensing, and decision-making technologies [10].

To address these challenges, modern autonomous systems increasingly rely on multi-sensor fusion, learning-based approaches, and adaptive motion planning algorithms. Visual-inertial odometry (VIO), and SLAM are examples of sensor-driven methods that enhance robustness in changing environments.

1.2.1 Global Positioning System

When it comes to the localization of the drone, the most popular and obvious solution is using the global navigation satellite system (GNSS), the most popular type of which is global positioning system (GPS). Other widely used systems are GLONASS, Galileo and BeiDou.

The accuracy of usage of GPS for UAV applications is proven by many projects and research [11] .While the principle of location estimation remains the same as it is implemented in daily used devices, there are some features of GPS usage in UAVs:

1. GPS might have a time offset in the signal, an error, or spoofing, what sig-

nificantly influence the flight of GPS-guided drone. The issue is resolved by creating special observers or neural networks, that are able to identify abnormal GPS signals [12].

2. GPS has quite low working frequency (up to 10 Hz), which is not usually enough for successful performance. That is why it is usually used as a correction data, than as a main information. For instance, it is widely combined with inertial measurement unit (IMU) [13].
3. UAVs can be programmed with virtual boundaries (geofences) using GPS coordinates to restrict flight zones (e.g., near airports or military areas).
4. Currently drones are widely used indoors or underground, which are GPS-denied environments. If the drone is GPS-guided it is not able to complete a task, hence there is a need for other navigation systems development.

Installing GPS modules in drones, the output signal type should be considered. The desired type of information is latitude and longitude, which may be either directly obtained from the GPS module or calculated from raw data, such as pseudorange (distance to each satellite) using the trilateration algorithm [14].

GPS is useful for the localization problem, as it can give a precise location of the drone on the map. It is a unique solution that can give the position with respect to the Earth, which makes it essential for the tasks, where the address of the target is known or the drone needs to fly large distances. However, it can not estimate the orientation of the UAV.

1.2.2 Inertial Navigation System

The only effective solution for the autonomous aircraft orientation estimation remains the IMU, which usually consists of the gyroscope, accelerometer, and magnetometer. It can either be used as part of the navigation system or as the only sensor in accordance with the UAV level of autonomy.

Inertial navigation system (INS) is one of the solutions for UAV navigation in GPS-denied environments. It provides the position and orientation of the drone with relativeness to the initial position. INS has two types of sensors, one of which is always IMU and another measures the movement of the drone in space, to determine the location of the drone. It can be either an optical flow sensors, cameras, distance sensors, etc. One of the solutions for how the data from the environment might be obtained was proposed in [15] and [16] as a vision-aided INS, which implies usage of landmarks, observed by camera. Analysis of the landmarks movement in image frames enables the estimation of rigid body movement.

The main disadvantage of INS is the measurements drift in time. While it is not crucial for the short flights (as measurements are corrected in the beginning of every flight), drift in time makes INS usage impossible for long-lasting tasks. In that case, the information from the environment is required to correct the measurements and continue the flight.

Using INS for drone localization, we assume that the operating environment is known in advance and static, as the changes in environment can not be sensed. With the precise initial location of the drone and a pre-existing map, path planning may be performed.

1.2.3 Indoor Positioning Systems

UAV localization in GPS-denied environments remains the challenging issue. For indoor application multiple solutions were developed, that allows to determine the volume of available space and the location of the UAV. The selection of an appropriate system depends on the specific application requirements, such as the size of the environment, acceptable positioning error, and power constraints. Some of the widely implemented approaches for indoor positioning, their response frequency and specific features are shown in Table 1.2.

As different technologies using different electro-magnetic waves have dif-

Table 1.2. Comparison of the indoor positioning systems for UAVs

Name	Response Frequency	Specific Features
Lighthouse Positioning System	30–34 Hz	• High precision; • Easy to transport; • Uses Valve SteamVR base stations (IR lasers); • Used for precise multi-UAV indoor flights [17].
Ultra-Wideband (UWB) Positioning System	100–200 Hz	• Uses RF waves (3.1–10.6 GHz); • Centimeter accuracy; • Good material penetrability; • Low transmission energy.
Bluetooth Navigation System	1–10 Hz	• Low-cost BLE beacons; • 2.4 GHz frequency; • Works up to 30 m; • Low power; • Scalable[18].
Motion Capture System	30–500 Hz	• Uses infrared waves; • Requires markers on UAV; • Sub-millimeter accuracy; • Expensive; • Needs external cameras; • Usually used as ground-truth.

ferent accuracy and price, the principle of their work is the same. The operation space must be equipped with base stations (or cameras for motion capture systems), the location of each is known. Each anchor measures the distance to the rigid body (in our case it is UAV) and sends the information to the center, where the final location is estimated. The center of processing is usually implemented as an additional server, which allows multiple drones to operate in one environment at the same time.

1.2.4 Visual-Inertial Odometry

Another greatly developed approach of the navigation in GPS-denied environments is visual-inertial odometry (VIO), which combines data from visual and inertial sensors to estimate the pose (position and orientation) of drone. This technique is widely used in applications when the map of environment is unknown and its creation is not required.

VIO estimates the location and orientation of the vehicle relative to the local starting position. This process is done by analyzing different image frames and comparing the movement of marks on images in time. In some sources VIO is considered as a computer vision technique [19, 20].

There are different approaches of fusing IMU measurements and estimations from camera are:

1. Multi- state constraint Kalman filter (MSCKF). This algorithm uses the geometric constraints between all the poses of the camera that observed a particular feature in the image. It shows the optimal result without 3D feature positions required [21].
2. Open keyframe-based visual-inertial SLAM (OKVIS). A keyframe-based VIO system using nonlinear optimization (sliding-window bundle adjustment) to tightly fuse camera and IMU measurements [22].
3. Semi-direct visual odometry (SVO). This algorithm is divided into three steps: sparse image alignment, relaxation, and refinement. 3D point on image frame are found based on minimization of the intensity difference of features[23].
4. Robust visual inertial odometry (ROVIO). This method simplifies the landmark selection by using points in the image, where the intensity changes considerably[24].
5. Monocular visual inertial navigation system (VINS-Mono). A monocular visual-inertial SLAM system using tightly-coupled nonlinear opti-

mization (sliding-window bundle adjustment) to fuse pre-integrated IMU measurements with tracked visual features. It includes robust initialization and loop-detection (pose-graph) modules for global consistency [25].

Precise time synchronization between the camera and IMU is critical in VIO. Even small delays can result in large pose errors due to the high dynamics of drone motion. Therefore, hardware-level synchronization and accurate camera-IMU calibration are prerequisites for reliable VIO performance.

1.2.5 Simultaneous Localization and Mapping

Simultaneous localization and mapping (SLAM) algorithms are widely used in the scenarios, when the pre-existing map of the environment is unavailable, however it is necessary for the successful performance. The primary objective of SLAM is to allow a robot or unmanned vehicle to build a map of an unknown environment while simultaneously estimating its position within that map.

To analyze the environment and create the map the following sensors are widely used:

1. Distance sensors (Sonar, LiDAR, ultrasonic sensors) are used for measuring the distance to surrounding objects or surfaces with high accuracy [26];
2. Cameras (RGB-D sensors, monocular, stereo and omnidirectional cameras) provide rich visual information that enables feature detection and depth estimation.

Processes, that are performed during SLAM can be divided into two groups as follows:

1. Front end: getting data from sensors, feature extraction, feature tracking (data association);
2. Back end: map estimation, data filtration (using Kalman-based filters), pose-graph optimization, loop closure detection.

SLAM algorithms vary according to the sensor used, estimation approaches, environment and the features of the task, UAV has to perform.

1.3 Sensor Fusion and Perception

Regularly, all autonomous systems have sensors, that analyses environment, which is either known or unknown. As UAVs need to track their state and parameters such as thrust, torque, speed of motors, all of them have sensors, that are working with these data. To get a precise pose and location of the drone, and have a high frequency of updates, two types of sensors must be combined. There are different approaches for fusing; however, the strategy remains the same. Its scheme is demonstrated on Figure 1.4.

Надається авторами за запитом

Figure 1.4. Multi-sensor fusion architecture

As both IMU and environment data based sensors (EDBS) have noise and/or bias, their measurements must be corrected before fusing. There are different approaches for this stage of filtering:

1. Low-pass and high-pass filters - suitable for scenarios where slow-changing motion is expected, or the bias should be eliminated;
2. Kalman filter - suitable for linear systems, allows to eliminate random values, as each measurement is compared with the previous one;
3. Extended Kalman filter - alternative for Kalman filter, implemented for nonlinear systems, that uses analytical linearization;

4. Unscented Kalman filter - nonlinear Kalman filter, that approximates the nonlinear function by applying is to the selected set of sample points[27].

For fusing the measurements from different sensors Madgwick algorithm [28], linear and nonlinear complementary filters are widely applied [29, 30].

1.4 Machine Learning Approaches

Implementation of the machine learning (ML) algorithms to the UAV attitude estimation is rapidly developing. Algorithms are used for data filtering and sensor fusion, and they allow to react to challenging situations and adapt to dynamic environments. The task for ML algorithms varies according to the used technologies.

One of the most popular ML approaches, implemented in UAV is deep learning (DL). Deep neural networks shows particularly great performance in the image processing, hence it is gaining popularity in mapping, VIO, detecting the obstacles and creating landmarks [31, 32]. It allows to perform the segmentation in image frames, what makes the path planning optimized, as the drone understands well sizes and forms of obstacles.

Attitude estimation algorithm is usually based on the Reinforcement Learning. It is used in the same time with traditional complementary filters for tuning the gains, what allow to adjust the weight for difference sensors in real time. This approach allows to eliminate random values and changes of the measurements, caused by external forces (for example, electro-magnetic field) [33].

In many scenarios ML enables the high accuracy estimation results. The main issue of the ML in UAVs is necessary large computational power, what increases the requirements for onboard devices. Recent developments in lightweight neural network architectures and edge computing devices aim to address this challenge, making real-time ML more feasible on resource-constrained platforms.

1.5 Justification for the Chosen Technologies of the Developed Device

Considering all possible applications for UAV attitude estimation, the selection of the system can be performed.

The main task of the project is to create a drone that, can operate in different environments, including indoor and GPS-denied environments, hence the GNSS or indoor positioning systems would be unsuitable for the project. The Inertial Navigation System, that contains IMU with gyroscope and accelerometer, optical flow sensor, that gives the movement along the axes x and y, and distance sensor for height measurement, was selected. The system allows drone to understand its movement with relativeness to the initial point. INS will provide the drone with the measurements of angular velocities, accelerations and movement, which are comprehensive to estimate the pose.

In this project map of the environment is not required, however drone needs to precisely understand its relative position. To secure accuracy multiple filters are applied. IMU measurements will be corrected with the extended Kalman filter, as we consider the UAV as a nonlinear system. Moreover, the measurements from optical flow, distance sensors and IMU will be further fused using linear complementary filter.

In this project mini UAV is considered, which time of flight does not exceeds 30 minutes, hence the possible time drift of INS is assumed not to influence the performance. Moreover, in mini UAV the computational power is limited, so all estimations need to be optimized.

Conclusions for Chapter 1

Developing a universal and reliable orientation system for unmanned aerial vehicles (UAVs) remains a relevant scientific and engineering challenge. This is due to the complex dynamics and nonlinear nature of UAVs, the broad range of tasks they perform, and the constantly changing and unpredictable environments in which they operate.

An analysis of various navigation systems and UAV localization algorithms reveals the following key criteria for an ideal orientation system:

1. Low weight of onboard instruments, enabling use across UAVs of various sizes;
2. Minimal power consumption, and thus minimal impact on flight duration;
3. High responsiveness: frequent data updates that ensure rapid reaction to changes in position;
4. Adaptability to environmental conditions;
5. Optimized computation algorithm;
6. Capability of autonomous error correction, reducing drift over time;
7. Low implementation cost;
8. Robustness to noise and interference;
9. High accuracy in position and orientation estimation;
10. Adaptability to different UAV types and configurations, ensuring universal applicability.

None of the currently analyzed systems fully meet all of these criteria. Therefore, navigation technologies and data processing methods are selected according to the drone type, the task it is designed for, and the operating environment.

This study analyzes how UAV type affects the feasibility of installing additional onboard devices and the formation of control matrices. Navigation systems suitable for different environments are proposed, including GPS, (INS), and indoor positioning systems. Localization algorithms such as (VIO) and (SLAM) are considered, as well as signal filtering techniques—specifically, Kalman filter-based methods and multi-sensor data fusion. As a result of this analysis, the optimal composition of an inertial navigation system and the mathematical methods to be used for UAV orientation system are identified.

CHAPTER 2. DESIGN OF A UAV ATTITUDE ESTIMATION SYSTEM

2.1 UAV Structural Diagram Development

In the previous section the functional features of the attitude estimation were defined. Hence, the structural sheme of the UAV with INS can be designed. It is demonstrated in Figure 2.1. The designed sheme is showing the main components of the UAV and the process of the attitude estimation, as the data got from ech step of the system is elaborated.

Надається авторами за запитом

Figure 2.1. Structural diagram of the UAV with the attitude estimation system

The acronyms used in Figure 2.1 represent the following elements:

- UAV - unmanned aerial vehicle, in this case, the object of control;
- CS - control system, which includes:
  - IMU - inertial measurement unit;
  - C1 - converter 1;
  - C2 - converter 2;
  - MC - microcontroller;
  - RB - regulation body;
  - AM - actuator mechanism (in this case, DC motors).

- OF - optical flow sensor;
- LD - semiconductor laser diode, in this case vertical-cavity surface-emitting laser;
- G - gyroscope;
- A - accelerometer.

To get to the desired position, the current state of the UAV has to be estimated.

The input variables for the UAV, obtained from the remote control include:

- x^d – desired coordinate along the x-axis;
- y^d – desired coordinate along the y-axis;
- z^d – desired coordinate along the z-axis;
- ϕ^d – desired roll angle;
- θ^d – desired pitch angle;
- ψ^d – desired yaw angle.

The output variables, which introduces the current state of the UAV include:

- x – actual coordinate along the x-axis;
- y – actual coordinate along the y-axis;
- z – actual coordinate along the z-axis;
- ϕ – actual roll angle;
- θ – actual pitch angle;
- ψ – actual yaw angle.

The estimation is performed by the feedback loop, which consists of the accelerometer A, gyroscope G and Optical flow sensor OP. The estimated variables include:

- $\hat{x}$ – actual coordinate along the x-axis;
- $\hat{y}$ – actual coordinate along the y-axis;
- $\hat{z}$ – actual coordinate along the z-axis;
- $\hat{\phi}$ – actual roll angle;
- $\hat{\theta}$ – actual pitch angle;

- $\hat{\psi}$ – actual yaw angle.

The important issue of that the actual and estimated variables differ because of the sensor‘s noise and bias, which are expected to be eliminated at the time of data filtering. The first stage of transformation of the sensors’ measurements and the communication buses are designed in the IMU and converters C1 and C2. The communication buses allow effective sending of data to the microcontroller MC, which processes the information, perform all filtration algorithms and send the appropriate commands to the regulation body RB. The regulation body changes the state of actuator mechanism AM, which changes the position and orientation of the UAV.

External forces, that may disturb the system are shown in Figure 2.1 as $f(t)$. The external sources include the wind, turbulence, electromagnetic field, and voltage spikes.

The errors between estimated and desired coordinates and angles are calculated as follows:

$$\tilde{x} = x^d - \hat{x} \tag{2.1}$$

$$\tilde{y} = y^d - \hat{y} \tag{2.2}$$

$$\tilde{z} = z^d - \hat{z} \tag{2.3}$$

$$\tilde{\phi} = \phi^d - \hat{\phi} \tag{2.4}$$

$$\tilde{\theta} = \theta^d - \hat{\theta} \tag{2.5}$$

$$\tilde{\psi} = \psi^d - \hat{\psi} \tag{2.6}$$

2.2 Mathematical Preliminaries

The orientation of the drone must be represented with relativeness to the inertial system. That's why two coordinate systems are introduced: inertial frame (usually ground-attached) - I, and body attached frame - B, which are shown in Figure 2.2. The UAV is assumed to be a rigid body, all further transformations are made to determine the pose (position and orientation) of frame B with respect to frame I.

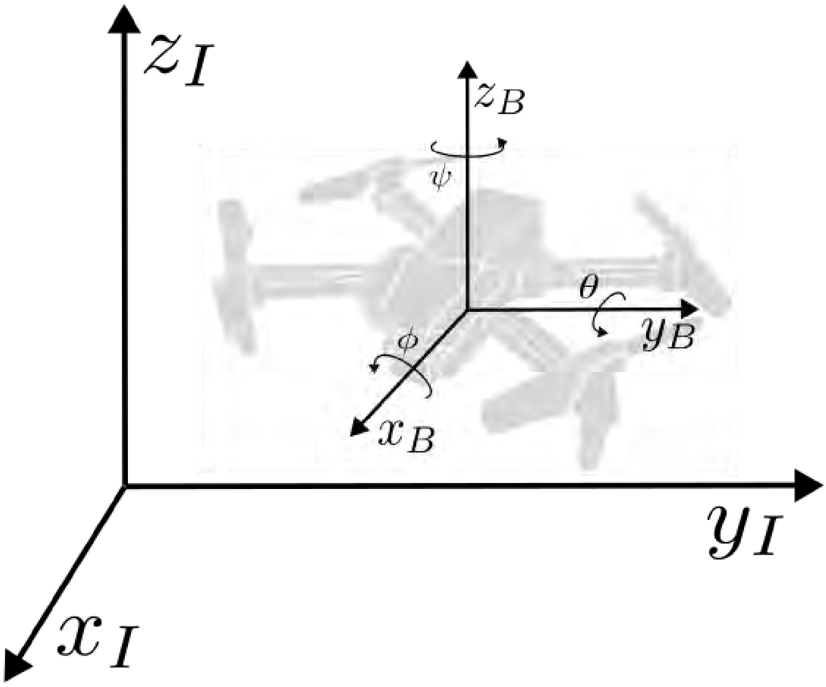

Figure 2.2. The representation of inertial and body-attached frames [29]

Three different approaches for orientation representation are considered. The first, and most popular is usage of Euler angles, which are ϕ is roll, θ is pitch and ψ is yaw or the tilt of B above x, y, and z respectively in an inertial frame I. They are particularly useful for high-level representation. Their main issue is that the usage of Euler angles can cause the uncertainty of the orientation estimation; hence, alternatives like rotation matrices and quaternions are widely used. In our case, the rotation matrix representation is used. as it allows to calculate desired torque and thrust, which can further be transformed to the voltage of each motor.

Rotation matrix can be divided to three parts, that shows the rotation of the rigid body with respect to axis x, y and z:

$$R_x = \begin{bmatrix} 1 & 0 & 0 \\ 0 & cos(\psi) & -sin(\psi) \\ 0 & sin(\psi) & cos(\psi) \end{bmatrix} \tag{2.7}$$

$$R_y = \begin{bmatrix} cos(\theta) & 0 & sin(\theta) \\ 0 & 1 & 0 \\ -sin(\theta) & 0 & cos(\theta) \end{bmatrix} \tag{2.8}$$

$$R_z = \begin{bmatrix} cos(\phi) & -sin(\phi) & 0 \\ sin(\phi) & cos(\phi) & 0 \\ 0 & 0 & 1 \end{bmatrix} \tag{2.9}$$

The total rotation matrix is the product of rotation matrices about each axis:

$$R = R_x R_y R_z = \begin{bmatrix} cos(\theta)cos(\phi) & sin(\phi)sin(\theta)cos(\phi) - cos(\psi)sin(\phi) & cos(\psi)sin(\theta)cos(\phi) + sin(\psi)sin(\phi) \\ cos(\theta)sin(\phi) & sin(\phi)sin(\theta)cos(\phi) + cos(\psi)sin(\phi) & cos(\psi)sin(\theta)cos(\phi) - sin(\psi)sin(\phi) \\ -sin(\theta) & sin(\psi)cos(\theta) & cos(\psi)cos(\theta) \end{bmatrix} \tag{2.10}$$

The rotation matrix is orthogonal, which means that,

$$R^{-1} = R^T \tag{2.11}$$

and

$$RR^T = I \tag{2.12}$$

where I is identity matrix.

2.3 Output Signals and Transformation of the Values

IMU used for the project consists of accelerometer and gyroscope. Hence, the output measurements that could be obtained are:

- Accelerometer outputs:
  - a_x – acceleration along X-axis
  - a_y – acceleration along Y-axis
  - a_z – acceleration along Z-axis
- Gyroscope outputs:
  - ω_x – angular velocity around X-axis
  - ω_y – angular velocity around Y-axis
  - ω_z – angular velocity around Z-axis

To convert the gyroscope measurements to Euler angles:

$$\phi_g = \frac{\omega_x}{f} = \int \omega_x \tag{2.13}$$

$$\theta_g = \frac{\omega_y}{f} = \int \omega_y \tag{2.14}$$

$$\psi_g = \frac{\omega_z}{f} = \int \omega_z \tag{2.15}$$

where f is the frequency of gyroscope measurements.

$$f = \frac{1}{T} \tag{2.16}$$

where T is the time difference between current and previous measurements in seconds.

To transform accelerometer measurements to Euler angles:

$$\theta_a = atan2(a_y, a_z) \cdot \frac{180}{\pi} \tag{2.17}$$

$$\phi_a = atan2(a_x, \sqrt{a_y^2 + a_z^2}) \cdot \frac{180}{\pi} \tag{2.18}$$

As the main acceleration, measured by accelerometer is gravity, which is not changed when yaw is adjusted, yaw can not be estimated with accelerometer.

To simplify future measurements, we will assume that the yaw angle can not be changed. If the yaw must be changed, the specific command is added to the user interface.

Another sensor, used in this project is optical flow sensor, which measures directly the movement with respect to x and y axis.

Output from Optical Flow Sensor (PMW3901):

- Δx - motion count on axis x since the last call;
- Δy - motion count on axis y since the last call.

Output for distance sensor:

- distance from the floor in millimeters - axis z.

2.4 Attitude Estimation

In this project, the task of attitude estimation is separated into 3 main steps:

1. Filtration of the bias and noise of the raw measurements;
2. Converting the raw measurements to the rotation matrix representation;

3. Defining the error between actual and desired pose of the drone.

2.4.1 Complementary Filter

Considering that in this work multiple sources of information about drone orientation are used, the sensor fusion of the measurements has to be done. The most common approach for this task is the complementary filter design. The complementary filter usually defines the weight for each source of data.

As it was previously discussed, the measurement of roll and pitch can be performed by two sensors in IMU: accelerometer and gyroscope. To increase the accuracy of the measurement the complementary filter is applied. The block diagram of complementary filter for pitch correction is demonstrated in Figure 2.3.

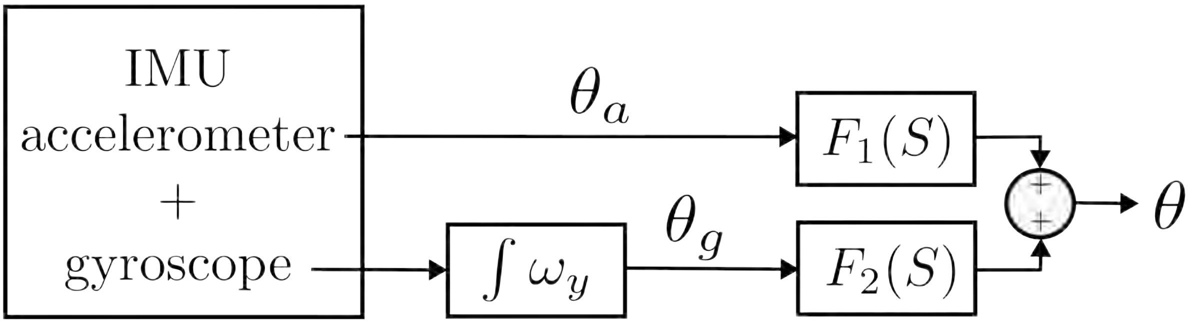

Figure 2.3. Complementary filter [29]

In the complementary filter a low pass filter is applied to minimize noise in measurements from an accelerometer:

$$F_1(s) = \frac{\tau}{\tau s + 1} \tag{2.19}$$

where τ represents the time constant, which determines the cutoff frequency and the relative contributions of the measurements. This parameter is fine-tuned during flight testing.

High-pass filter is utilized to eliminate gyroscope bias:

$$F_2(s) = \frac{s}{\tau s + 1} \tag{2.20}$$

The sum of the filters must result in 1:

$$F_1(s) + F_2(s) = 1 \tag{2.21}$$

The resulting equation for pitch is designed as follows:

$$\theta(s) = \frac{\tau}{\tau s + 1} \cdot \theta_a(s) + \frac{s}{\tau s + 1} \int \omega_y(s) ds \tag{2.22}$$

The resulting equation for roll is designed in the same way:

$$\phi(s) = \frac{\tau}{\tau s + 1} \cdot \phi_a(s) + \frac{s}{\tau s + 1} \int \omega_x(s) ds \tag{2.23}$$

Yaw estimation requires fusion of data from magnetometer and gyroscope [29]. As the magnetometer is not used in this project, yaw is estimated using only gyroscope data. The extended Kalman filter is applied.

2.4.2 Extended Kalman Filter

Fusing different sources helps us to get rid of the accelerometer noise and gyro bias, however it can not eliminate random values. For this issue Kalman Filters are widely used. One of the most popular of them is Extended Kalman Filter, which is working with nonlinear systems by applying linearization algorithms.

The filtration process can be divided into the following stages:

1. Initialization;
2. Prediction;
3. Update.

The initialization is performed in the beginning of every flight, and we will assume that first measurements obtained from sensors are correct. The initialization data are: x_0 - first measurement, and P_0 - initial covariance matrix, that represents initial uncertainty about the estimation.

For the attitude estimation of the designed UAV the initial covariance matrix has the following values:

- position uncertainty - 1 mm;
- angular velocity uncertainty - 0.01 rad/s;
- orientation uncertainty - 0.01 rad.

At the time of practical implementation the values might be tuned according to the behavior of the UAV.

In the step of prediction two values are calculated: measurement and covariance. In all further equations index k denotes the cycle of extended kalman filter algorithm.

Predicted measurement is calculated as follows:

$$x_{k|k-1} = f(x_{k-1|k-1}, u_k) + \omega_k \tag{2.24}$$

where $f(x_{k-1|k-1}, u_k)$ is a nonlinear state transition function, ω_k is a Gaussian noise and u_k is a control signal.

The linearization is performed by computing the Jacobians for nonlinear function:

$$F_k = \left.\frac{\partial f}{\partial x}\right|_{x=\hat{x}_{k-1|k-1}, u} \tag{2.25}$$

The predicted covariance of the linearized system:

$$P_{k|k-1} = F_k P_{k-1|k-1} F_k^T + Q_k \tag{2.26}$$

where Q_k is process noise covariance.

In the update step the actual measurement from sensor is updated at the same time with all gains, used in the algorithm.

Corrected measurement from the sensor:

$$z_{k|k-1} = h(x_{k|k-1}) \tag{2.27}$$

where $g(x_k)$ is a nonlinear measurement function. The linearization is applied:

$$H_k = \left.\frac{\partial f}{\partial x}\right|_{x=\hat{x}_{k-1|k-1}} \tag{2.28}$$

Corrected residual covariance:

$$S_k = H_k P_{k|k-1} H_k^T + R_k \tag{2.29}$$

where R_k is

Corrected Kalman gain:

$$K_k = P_{k|k-1} H_k^T S_k^{-1} \tag{2.30}$$

Corrected prediction:

$$\hat{x}_{k|k} = \hat{x}_{k|k-1} + K_k(z_k - z_{k|k-1}) \tag{2.31}$$

where z_k is a raw measurement from sensor. Corrected covariance:

$$P_{k|k} = P_{k|k-1} - K_k S_k K_k^T \tag{2.32}$$

2.5 Designing the Torque Control

Torque τ design must lead to decreasing the error between desired and estimated orientation parameters.The calculation of errors in Euler angles are demonstrated in equations 2.4, 2.5 and 2.6.

Total torque is divided into three components τ_x , τ_y and τ_z which are representing the desired torque in three axes x, y and z respectively.

$$\tau = \begin{bmatrix} \tau_x \\ \tau_y \\ \tau_z \end{bmatrix} \tag{2.33}$$

The desired torque can be obtained from the PID (proportional–integral–derivative) controller. For example, the equation for τ_y will be as follows:

$$\tau_y = k_p^\theta \tilde{\theta}(t) + k_i^\theta \int_0^T \tilde{\theta}(t)\, dt + k_d^\theta \frac{d\tilde{\theta}(t)}{dt} \tag{2.34}$$

where k_p, k_i and k_v are nonnegative proportional, integral and derivative gains respectively.

$$\frac{d\tilde{\theta}(t)}{dt} = -\dot{\theta} = -\omega_x \tag{2.35}$$

However, as a derivative of the error in Euler angle is the angular velocity (equation 2.35), which is obtained directly from gyroscope, the PIV (proportional–integral–velocity) controller is used in this project. The block diagram of the PIV controller is shown in Figure 2.4.

Gains introduced in Figure 2.4 are as follows,

$$K_p = \begin{bmatrix} k_p^\theta & 0 & 0 \\ 0 & k_p^\phi & 0 \\ 0 & 0 & k_p^\psi \end{bmatrix} \tag{2.36}$$

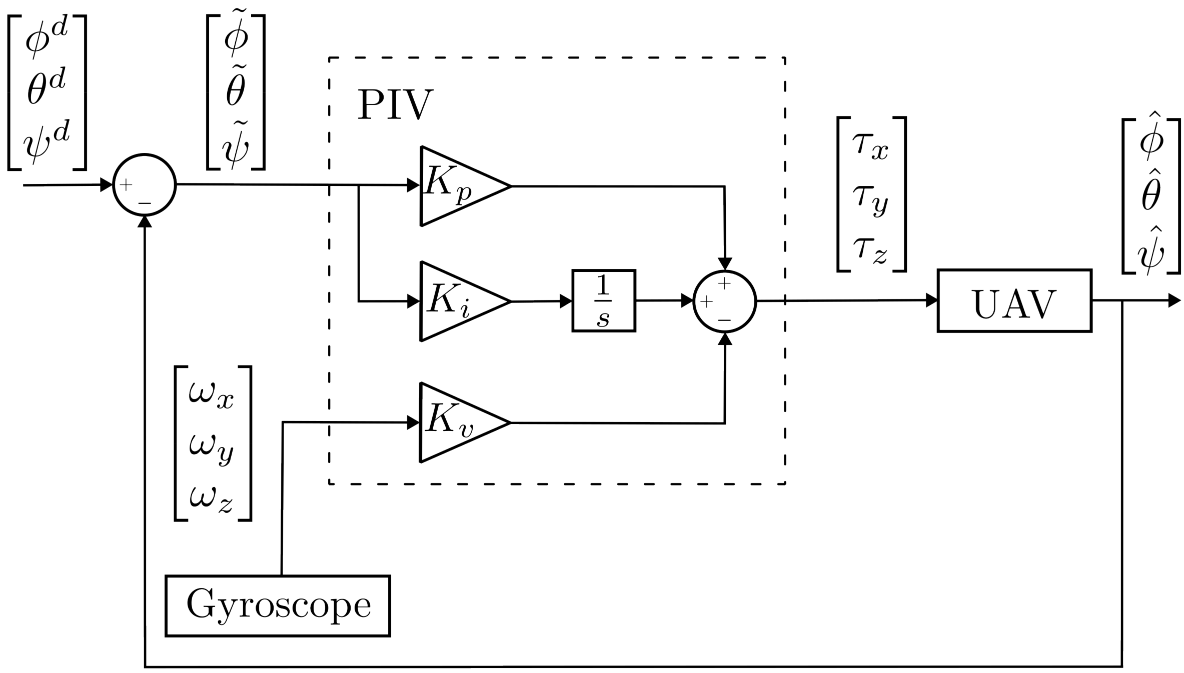

Figure 2.4. PIV for torque design

$$K_i = \begin{bmatrix} k_i^\theta & 0 & 0 \\ 0 & k_i^\phi & 0 \\ 0 & 0 & k_i^\psi \end{bmatrix} \tag{2.37}$$

$$K_v = \begin{bmatrix} k_v^\theta & 0 & 0 \\ 0 & k_v^\phi & 0 \\ 0 & 0 & k_v^\psi \end{bmatrix} \tag{2.38}$$

where k_p, k_i and k_v are nonnegative proportional, integral and velocity gains respectively.

The equations for torque with respect to axes x, y and z are as follows:

$$\tau_x = k_p^\phi \tilde{\phi}(t) + k_i^\phi \int_0^T \tilde{\phi}(t)\, dt - k_v^\phi \omega_x \tag{2.39}$$

$$\tau_y = k_p^\theta \tilde{\theta}(t) + k_i^\theta \int_0^T \tilde{\theta}(t)\,dt - k_v^\theta \omega_y \tag{2.40}$$

$$\tau_z = k_p^\psi \tilde{\psi}(t) + k_i^\psi \int_0^T \tilde{\psi}(t)\,dt - k_v^\psi \omega_z \tag{2.41}$$

Integral boundaries are reset when time reaches the limit to eliminate undesired noise.

2.6 Designing the Total Thrust

Another important parameter of the flight is the total thrust T, got from all four motors. This value will define the hight of the flight, and the possibility to move to desired position.

The aim of the control is to make error between desired and actual position tend to zero:

$$\tilde{P} = P_d - P \to 0 \tag{2.42}$$

where $\tilde{P}$ is an error, P_d - desired position, and P is actual position .

In the inertial frame the Newtons second law, written for the quadrotor UAV looks as follows:

$$ma = mge_3 + TR_d^T e_3 \tag{2.43}$$

where m - mass of the drone, a - acceleration of the movement, R_d - rotation matrix of the desired orientation, and e_3 - unit vector on axis z. The acceleration - is the second derivative of the position error.

$$a = \dot{\tilde{v}} = \ddot{\tilde{P}} = \ddot{P}_d - \ddot{P} \tag{2.44}$$

We assume that the desired acceleration is 0, hence

$$a = 0 - \ddot{P} = 0 - \dot{v} = \mu \tag{2.45}$$

where μ is control input.

Hence, the equation 2.43 can be transformed to the following:

$$\mu - ge_3 = \frac{T}{m} R_d^T e_3 \tag{2.46}$$

If the norm of each part is taken:

$$||\mu - ge_3|| = ||\frac{T}{m} R_d^T e_3|| \tag{2.47}$$

$$||\mu - ge_3|| = ||\frac{T}{m}|| \cdot ||R_d^T e_3|| \tag{2.48}$$

where $||R_d^T e_3|| = 1$, hence

$$T = m||\mu - ge_3|| \tag{2.49}$$

2.7 Extracting Voltage for Each Motor

While the thrust and torque are defined, the control input has to be defined. As we have the DC motors, the control input must be transformed to four voltages - one for each motor.

As it was stated previously, the control matrix M depends on the form of the drone. The frame of the developed drone is demonstrated in Figure 2.5.

Based on the classification, given in section 1.1.1 the developed drone is a quadrotor H-frame UAV. The control matrix for this type will have the following form:

Figure 2.5. Frame for the developed UAV

$$M = \begin{bmatrix} 0 & k & 0 & k & 0 & k & 0 & k \\ -b & kL_y & b & kL_y & -b & -kL_y & b & -kL_y \\ 0 & -kL_x & 0 & kL_x & 0 & kL_x & 0 & -kL_x \\ -kL_y & -b & -kL_y & b & kL_y & -b & kL_y & b \end{bmatrix} \tag{2.50}$$

where k and b and distances L_y and L_x are shown in Figure 2.6.

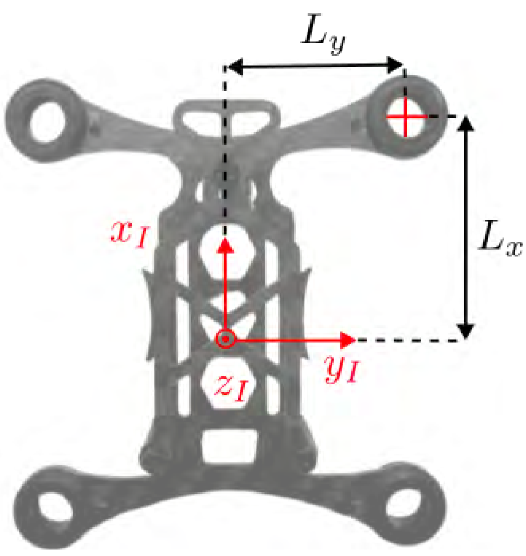

Figure 2.6. Distances L_x and L_y

$$
\begin{bmatrix} T \\ \\ \tau \end{bmatrix} = M \begin{bmatrix} \omega_1^2 \\ \\ \omega_2^2 \\ \\ \omega_3^2 \\ \\ \omega_4^2 \end{bmatrix} \tag{2.51}
$$

where $\omega_1, \omega_2, \omega_3$ and ω_4 are angular velocities for each motor.

For voltage-controlled motors:

$$
V_i = \frac{R_a}{k_m k_g} \tau_i + k_m k_g \omega_i \tag{2.52}
$$

where R_a - resistance of motor, k_m - motor torque-constant, k_g - gear ratio [34].

Conclusions for Chapter 2

The most important part of the quadrotor attitude estimation is filtering data and fusing measurements from different sensors, as the accuracy of the position and orientation influences the stability of the drone. In this section we analyzed the data, obtained from IMU, optical flow sensor and distance sensor to create the optimal filtration algorithm for INS. The structural diagram was created, which demonstrates the transformation of the position and orientation parameters transformation.

Based on the quadrotor dynamics, the algorithm of designing torque and thrust was performed, which enabled the calculation of the voltage for each DC motor. In this chapter the frame of the designed UAV is presented, as its geometry influences the formation of the control matrix M.

CHAPTER 3. DEVELOPMENT OF UAV ARCHITECTURE FOR ATTITUDE ESTIMATION

3.1 UAV Fuctional Diagram Development

Based on a detailed analysis of all component outputs, a functional diagram can be constructed to illustrate the primary roles and interactions of each subsystem within the overall architecture. This diagram serves to clarify how data flows between modules and how control functions are distributed across the system. It is shown in Figure 3.1.

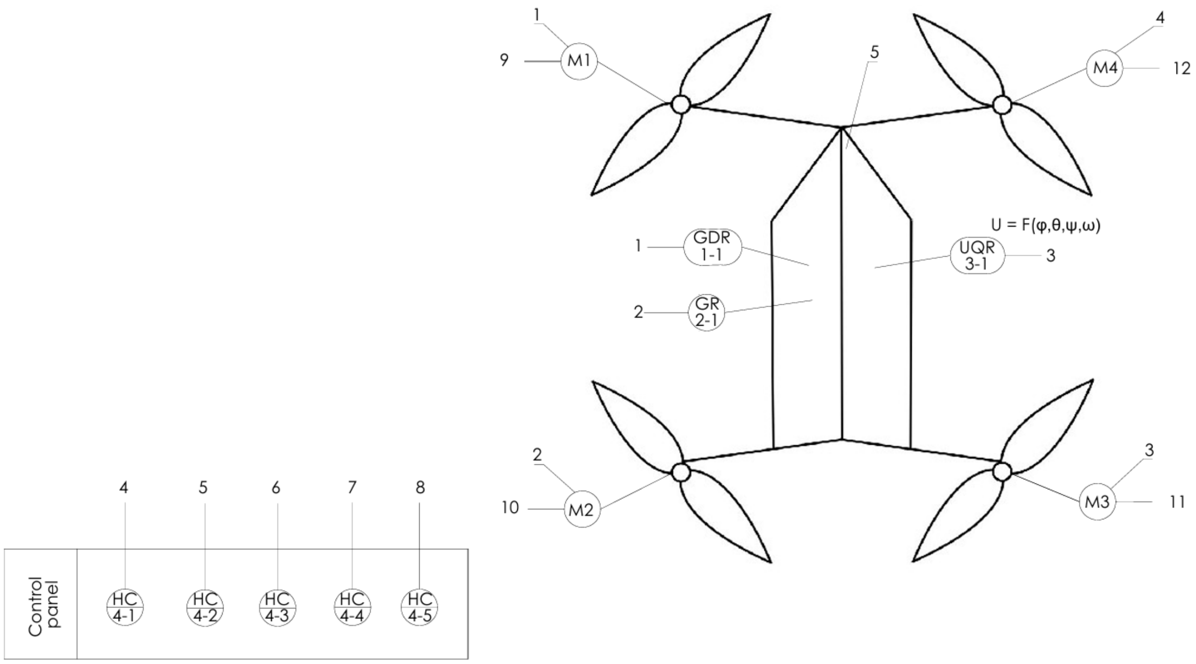

Figure 3.1. Functional diagram of the UAV with the attitude estimation system

The designations, used on the functional diagram represent the following elements:

- GDR - registration of position change (displacement);
- GR - registration of position measurement;
- M1 - 4 - DC motors;
- UQR - a device for measuring several heterogeneous quantities, in this case, angles and accelerations along the x, y, and z axes;

- HC - equipment for manual remote control, in this case - buttons.

Data from the elements, that either measures the state of the UAV or defines the desired pose, is transferred to the micro controller for processing. The type of desired data and time for recording are shown in Figure 3.2.

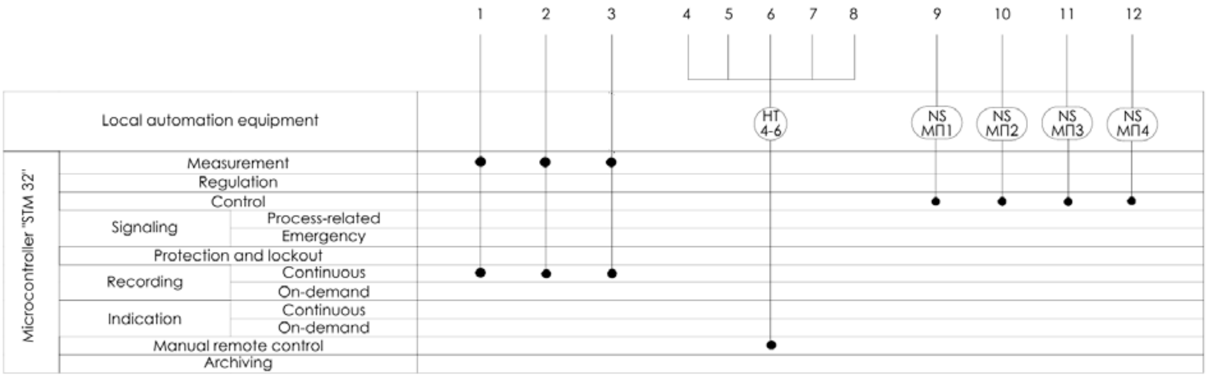

Figure 3.2. Functional diagram of the microcontroller-based UAV attitude estimation system

The local automation equipment, used in Figure 3.2 are as following:

- HT - a device for remote transmission of signals from the manual control panel, in this case, a device for obtaining the desired coordinate of the drone from the control panel ;
- NS - equipment for controlling the electric motor.

3.2 Electronics

The important part of the project is the electronic component selection, as multiple sensors are used and large amount of data has to be transferred and process. To understand the communication buses, used in the project, the component selection is performed before the electrical schematic diagram design.

3.2.1 Micro-controller

The most important part of every UAV is the contorller. In this project the micro-controller STM32 blue pill is used. The microprocessor is STM32F103C8T6.

The selection of this equipment for the project was made based on the following criteria:

- High speed of data processing, as it is crusial for the UAV flight;
- Possibility to use multiple sensors with I^2C and SPI communication interfaces;
- More than 30 GPIOS, as they will be required for the components connection;
- Small and lightweight;
- Low power consumption;
- Affordable cost.

Figure 3.3 represents the pinout diagram of the STM32 blue pin. It demonstrates that microcontroller has enough GPIOS (37) and it is possible to use different communication interfaces. To be more detailed, 2x I^2C, 3x USART/UART, 2x SPI, 1x USB, 1x CAN. Moreover, it has 10x analog inputs and 20x PMW outputs.

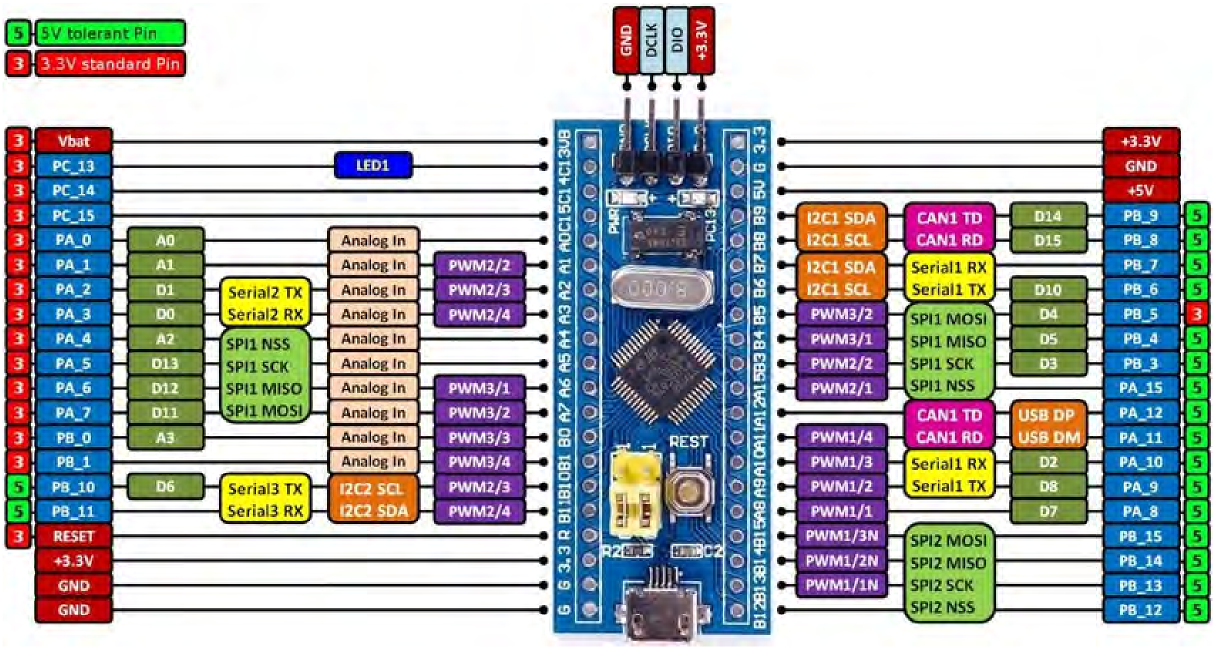

Figure 3.3. STM32 pinout diagram [35]

The STM32 weight is 8g, and it has the low power mode available. It price varies from 25 USD to 30 USD and there are many unofficial counterfeits on the market, that could be purchased for 4 - 10 USD. What makes it a perfect microcontroller, for this project.

Other specifications, that might be useful of should be considered furhter for this project are:

- Core: ARM Cortex-M3 (32-bit, RISC);
- Clock Speed: Up to 72 MHz;
- Flash Memory: 64 KB;
- SRAM: 20 KB;
- Operating Voltage: 2.0V – 3.6V;
- Timers: 7 (including advanced PWM features);

3.2.2 Communication Method Selection

An important input parameters for the UAV are the desired position and orientation, that has to be obtained from the remote control. To get the information from remote control, communication method must be provided. The information from the remote control is transfered by radio waves.

Regularly, the radio modules require antennas, which have relatively huge weight, but they increases the possible distance for communication. In our case long distance is not required, however the weight is crucial, as we are working on the mini UAV (Table 1.1). That is why the NRF24L01+ is used. It has onboard antenna, which operates on frequency 2.4 GHz, and can operate in low power mode.The photo of the used radio module is demonstrated in Figure 3.4.

The information from NRF24L01+ is transferred to the microcontroller through SPI interface. The required voltage for operating is 3.3 V.

Figure 3.4. Radiomodule NRF24L01+

3.3 Navigation System Formation

As it was described previously, the drone is equipped with the INS, which consists of IMU, optical flow sensor and distance sensor (semiconductor laser diod). The combination of these sensors will give the position and orientation in 3 axes with relativeness to the initial position.

3.3.1 Inertial Measurement Unit

MPU6050 The required sensors for IMU is 3-axis accelerometer and 3-axis gyroscope. They are provided in the MPU6050, which does not have any embedded fusing and filtration algorithms, what enables implementing the mathematical transformations discussed in section 2.4. MPU6050 is demonstrated in Figure 3.5.

Specifications, important for further work:

- Gyroscope full-scale range: ± 250, ± 500, ± 1000, and $\pm 2000°/$s;
- Accelerometer full-scale range: $\pm 2g$, $\pm 4g$, $\pm 8g$, and $\pm 16g$, where g - gravitational acceleration;
- 16-bit ADCs for both gyroscope and accelerometer measurements;
- I^2C interface, supporting standard and fast modes (up to 400 kHz).
- Operating voltage range: 2.375 V to 3.46 V;

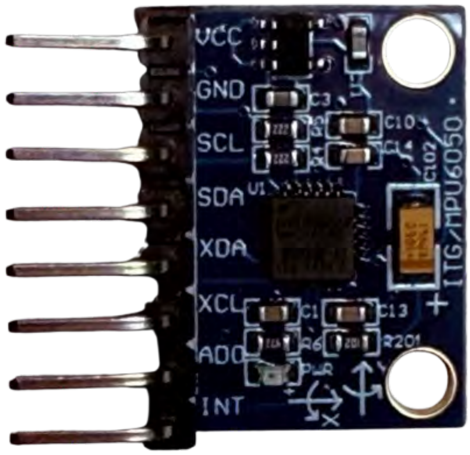

Figure 3.5. MPU6050

- Low power mode;
- Weight: 1.8 g;

3.3.2 Optical Flow Sensor

Optical flow sensor provides the information about movement with relativeness to axes x and y. This type of sensors is nor popular on the market, as there are only few applications for them. The one widely used for UAVs is PMW3901. Modules developed for this chip are usually designed for specific flight conroller, which limits the possibilities of getting raw information. We will use the Pimoroni PMW3901 sensor, which is designed for Rasberry Pi and Arduino, hence the information coud be obtained for STM32 as well. The sensor is demonstrated in Figure 3.6.

There are some limitations and specific features of the sensor, that should be considered for further design:

- Detects motion by tracking texture on the ground (optical flow), hence flying above the monochromatic surface is undesired;
- Measures motion in X and Y directions (no Z-axis measurement);
- Works at high frame rates: up to 120 frames per second;

Figure 3.6. Pimoroni PMW3901 sensor

- Field of view: 42°;
- SPI communication interface for fast data transfer;
- Typical working distance: 80 mm to 2000 mm from surface;
- Low power consumption.

It is important to mention that two of the already selected components use SPI communication interfaces. That is why because of the limitations of the STM32, all further elements should work with other protocols.

3.3.3 Distance Sensor

The parameter, that is not measured by the previous components, but is crucial for attitude estimation is the height of flight or the position in relativeness to the axis z. It could be measured by the distnce sensors. As the speed of obtaining information might be crucial for the flight, it was decided to use a distance sensor, that is wirking with optical waves. To be more specific, the VL53L0X V2 Time of Flight distance sensor was selected (Figure 3.7).

Key specifications:

- Measures absolute distance using Time-of-Flight (ToF) principle;
- Laser-ranging sensor with Class 1 eye-safe 940 nm VCSEL (Vertical cavity surface emitting laser);

Figure 3.7. VL53L0X V2 time of flight distance sensor

- Accurate distance measurement regardless of target reflectance;
- Measurement range: up to 2 meters;
- I^2C interface for communication;
- Compact and low-power operation;
- Compatible with Arduino, Raspberry Pi, and STM32.

3.4 Motors Selection

The designed UAV can only operate on the electrical motors due to its small sizes [1]. Moreover, only DC motors can be implemented as brushless motors requires high operational power, are more heavy and requires additional ESC for each motor.

DC motors, selected for this project are coreless motor 8520 (Figure 3.8), two clockwise and two counterclockwise, as propellers have to rotate in different directions to eliminate undesired torque.

Chosen motors have the following parameters:

- Dimensions: 8.5 mm × 20 mm;
- Voltage: 3.7 V;
- Shaft diameter: 1 mm;
- Operating voltage range: 3–4.2 V;
- Operating current: 150 mA;
- Weight: 5 g.

Figure 3.8. Mini DC motor 8520

3.4.1 Motor Driver

The speed of DC motors is controlled by voltage, which is regulated by motor drivers. In this case, motor driver DRV8835 is used, which can work simultaneously with two motors, adjusting the speed of each of them. Hence, in the application of quadrotor UAV two DRV8835 are required. The photo of DRV8835 is demonstrated in Figure 3.9.

Figure 3.9. Motor driver 8835

Key specifications:

- Maximum output current: 1.5 A
- Motor-operating supply voltage range: 0 V to 11 V
- Logic supply voltage range: 2 V to 7 V
- Package: 12-DIP

3.5 Power Source System

All components are operating on electrical current, hence the battery is required. The only component that must be connected to the battery directrly is the microcontroller. As it was mentioned previously, STM32 operating voltage can be in range 2 - 3.6 V, hence the battery with the nominal voltage 3.7 v. Long time flight is not required in this project, hence there are no exact requirements for the nominal capacity battery.

Lithium polymer battery with capacity 700 mAH was selected, as it keeps a perfect balance between capacity and weight, which is 15 g. The chosen battery is shown in Figure 3.10.

Figure 3.10. Lithium polymer battery

3.5.1 Battery Charging Board

Battery charging board is required to charge a battery and have an opportunity to continue a flight. The charging board TP4056 Type-C was selected (Figure 3.11).

Key specifications:

- Input voltage: 4.5 V – 5.5 V;
- Final charging voltage: 4.2 V;
- Discharge protection voltage: 2.4 V;
- Charging current: 1 A;
- Charging connector: Type-C;
- Operating temperature range: –10 °C to +85 °C;
- Dimensions: 27.75 mm × 17.25 mm.

Figure 3.11. Battery charging board TP4056 Type-C

3.6 UAV Electrical Schematic Diagram Development

When all components are selected and their communication interfaces are known, the electrical schematic diagram can be designed. It is shown in Figure 3.12. Designators in the diagram represent the following elements:

- DD1 and DD7 - motor driver DRV8835;
- DD2 - radio module NRF24L01;
- DD3 - microcontroller STM32 blue pill;
- DD4 - MPU6050;
- DD5 - distance sensor VL53L0X;
- DD6 - optical flow sensor Pimoroni PMW3901.

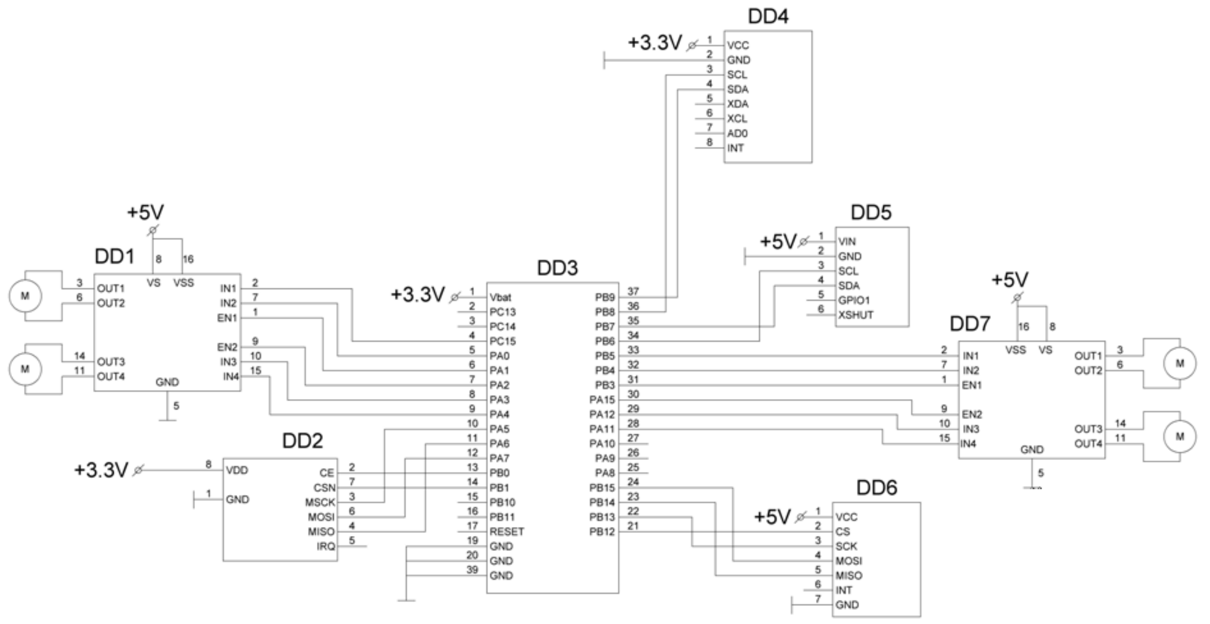

Figure 3.12. UAV Electrical Schematic Diagram

The communication interfaces, considered in the diagram:

- SPI between STM32 and radiomodule NRF24L01+ (DD22)
- SPI between STM32 and Pimoroni PMW3901 sensor (DD65)
- I^{2}C between STM32 and MPU6050 (DD43)
- I^{2}C between STM32 and VL53L0X V2 time of flight distance sensor (DD54)

Additionally, two DRV8835 dual h-bridge motor drivers (DD1 and DDT) are used to control four DC motors. They are powered by a +3.7V supply and receive control signals from the STM32.

This architecture enables real-time control of actuators, inertial and optical-based navigation, and wireless data transmission, making it suitable for applications in UAVs.

Conclusions for Chapter 3

In this chapter the selection and justification of all components for the quadrotor UAV with attitude estimation system was performed. All chosen equipment is available on the market, what makes the system affordable and accessible for users.

The main functionality of the each component was analyzed, based on which the functional diagram was created. The diagram shows logical roles, signal flow and timing of data recording, what is crucial for attitude estimation algorithm.

Special emphasis was placed on the communication protocols and their integration with the STM32 microcontroller, which serves as the central processing unit of the system. The electrical schematic diagrams were developed, which provides detailed insight into the wiring, pin configuration, and power distribution.

CHAPTER 4. SOFTWARE DEVELOPMENT FOR THE UAV ATTITUDE ESTIMATION SYSTEM

4.1 Algorithm Design

The operational algorithm for drone with attitude estimation system, which is working based on the INS, is demonstrated in Figure 4.1.

Надається авторами за запитом

Figure 4.1. Algorithm of the UAV with attitude estimation system operation

There are four conditional blocks. The first conditional block "Battery level acceptable" checks the safety of the flight and ensures that the drone will not fall after taking off because of the critical energy resources. Other conditional blocks check the existence of the new commands from remote control that will change the desired position. If new commands are not received, the drone assumes that the desired position is the same as the last estimated, what will ensure the stability of the flight.

Another important stage of the, is the measurement collection from sensors. It is crucial to collect all data in the shortest possible time, so we can assume that the information we are getting is from one position and orientation. That is why we propose to firstly collect all raw measurements, and after that process them by making all required transformations and applying filters.

4.2 Desired Position and Orientation Estimation

One of the steps for the successful operation of the drone is to correctly determine the desired position and orientation, as they influence the further algorithm of operation.

The operator has five buttons on the remote control, which means the following actions:

- TAKE OFF/LAND – start or end of the mission;
- FORWARD – increasing in x;
- BACKWARD – decreasing in x;
- LEFT – increasing in y;
- RIGHT – decreasing in y.

In this project we assume that the yaw is not changing, what eliminates the uncertainty in the torque design. Moreover, we do not add the commands UP and DOWN, as these actions does not require complex changes in drone orientation. To be more specific, buttons UP and DOWN would only influence the total thrust.

Changing the yaw leads only to the orientation modification, without influencing the position. It can be adjusted by changing the torque τ_z, using the equation 2.41. The discussed buttons, that are not implemented in this project, can be easily added in further modifications.

The commands will cause the following changes in the Euler angles, what will result in the formation of the desired rotation matrix:

- TAKE OFF: $z^d = \hat{z} + z_i$, where z_i is the height of the initial point;
- LAND: $z^d = \hat{z} + h$, where h is the height of the flight;
- FORWARD: $\phi^d = \hat{\phi} + \Delta\alpha$;
- BACKWARD: $\phi^d = \hat{\phi} - \Delta\alpha$;
- LEFT: $\theta^d = \hat{\theta} + \Delta\alpha$;
- RIGHT: $\theta^d = \hat{\theta} - \Delta\alpha$;

where $\Delta\alpha$ initially equals to 0.01 rad, but may be tuned based on the UAV performance and desired speed of flight.

4.3 Implementation of the Attitude Estimation Algorithms

To make the code more clear to create, read and debug, we are using structured data types for naming all the variables with the names used in equations in chapter 2. The defined types of variables are shown in Table 4.1

4.3.1 Pre-Transformation of the Measurements form Sensors

To transform the measurements from IMU to the Euler angles, equations 2.13, 2.14, 2.15,2.17 and 2.18 are used. In this project they are implemented in the following function:

```
angles measurements_to_angles(MPU6050_Data data, float frequency)
{
 angles converted_data;
 float rad_to_deg = 57.2957795131;

 converted_data.phi_a = atan2f(data.accel_y, data.accel_z) *
```

Table 4.1. Variables used for attitude estimation, using structured data types

List name	Application	Variables in the list
MPU6050_Data	Raw IMU measurements	• int16_t accel_x; • int16_t accel_y; • int16_t accel_z; • int16_t gyro_x; • int16_t gyro_y; • int16_t gyro_z.
angles	Angles, calculated from accelerometer and gyroscope measurements	• float phi_a; • float theta_a; • float phi_g; • float theta_a; • float psi_a;.
angles_filtered	Angles, filtered from IMU measurements by complementary filter	• float phi; • float theta; • float psi.

```
    rad_to_deg ;
 converted_data.theta_a = atan2f(data.accel_x, sqrtf(data.accel_y *
    data.accel_y + data.accel_z * data.accel_z)) * rad_to_deg;
 converted_data.phi_g = data.gyro_x / 131.0 /frequency ;
 converted_data.theta_g = data.gyro_y / 131.0 /frequency;
 converted_data.psi_g = data.gyro_z / 131.0 /frequency;

 return converted_data;
}
```

The transformation of the values, obtained from Pimoroni PMW3901 sensor to milimeters is performed by the function flow.readMotionCount(deltaX, deltaY) , which can be obtained from the library Bitcraze_PMW3901.

VL53L0X V2 gives distance in millimeters by applying the function VL53L0X _PerformSingleRangingMeasurement() , hence the pre-transformation is not required. The functions for this sensor may be found in the library vl53l0x_api.

4.3.2 Complementary Filter Implementation

The complementary filter is the important part of the algorithm, as it allows fusing the data. Mathematical operations used for the complementary filter are demonstrated in section 2.4.1. The implementation of the filter in this project is as follows:

```
angles_filtered complementary_filter(angles converted_data)
{
 angles_filtered filtered_data;
 float f_1 = 0.95;
 float f_2 = 1 - f_1;

 filtered_data.phi = f_1 * converted_data.phi_a +
    f_2 * converted_data.phi_g ;
 filtered_data.theta = f_1 * converted_data.theta_a +
    f_2 * converted_data.theta_g ;
 filtered_data.psi = converted_data.psi_a;

 return filtered_data;
}
```

The coefficients f_1 and f_2 illustrate the weight of the accelerometer and gyroscope measurements respectively. In this case we initially trust the accelerometer data more, however the coefficients might be tuned further based on the UAV performance.

Conclusions for Chapter 4

This chapter demonstrates how the algorithm, described in chapter 2 is implemented in the program for hardware, selected in chapter 3.

First stage of the algorithm is the estimation of the desired position and orientation, based on the commands from the remote control. In this chapter we discussed the commands is project and how they would influence the desired pose.

Sensor data processing was carefully implemented using structured data types, which improve code readability and maintainability. The transformation of raw IMU data into Euler angles allows for real-time feedback on the drone's orientation. Furthermore, a complementary filter was applied to fuse accelerometer and gyroscope data, balancing short-term stability with long-term accuracy. The filter parameters are designed to be tunable, making the system adaptable to different flight dynamics or environmental conditions.

The chosen sensors have a well-developed community, which resulted in the convenient libraries that may be effectively used in this project. To be more specific, the pre-developed libraries are used for optical flow and distance sensors.

CONCLUSIONS AND FUTURE DIRECTIONS

In this work the quadrotor attitude estimation system was designed. For this task different systems and algorithms for position and orientation estimations were analyzed in the chapter 1. The different environments for UAV performance were covered: outdoor, indoor, observable, partially observable, unknown. As possible environments of operation and mass of equipment depends on the size and type of UAV, the classification was performed.

After the detailed analysis we decided to use INS in this project, which consists of IMU, optical flow sensor and distance sensor. The designed system output is 3-axes position and orientation.

Usage of the different equipment requires measurement‘s filtration and sensor fusion, mathematical operations of which was discussed in chapter 2. For this task we analyzed the raw data we are getting from each sensor, made their pre-transformation and designed the structural scheme of the UAV with attitude estimation system. Two filters were used in this work: extended Kalman filter, which cancels the noise, and complementary filter, that fuses data from different sensors. Moreover, the algorithm to transform the errors between estimated and desired pose to the low-level commands for actuators are demonstrated. In our case, the input for actuators is voltage, as the DC motors are used.

In the chapter 3 the functions for each component of the designed UAV were analyzed and summed up in functional diagram, which illustrated the data flow in the system and timing for data recording. Based on the fact, that all components require transferring big amount of data to the microcontroller, and hence use different communication interfaces, the careful selection of the components was performed. Other features of the integral circuits, that were important for this diploma project are: operating voltage, measurement range and environment conditions, required for successful operation.

The main computing center is STM32, which was selected based on the supported communication protocols, power consumption, weight and size. An electrical schematic was designed to demonstrate interconnections between components, considering the STM32 pinout features.

As a result of this project the mini UAV, which is able to operate with only high-level commands from the remote control and autonomously define the position and orientation in the space, was designed. The drone is able to operate in pre-known environment, and defines position and orientation with respect to the initial state. This work lays a strong foundation for future development in UAV autonomy. Possible future directions of improvement include localization and mapping tasks, which will require additional equipment, such as cameras or indoor positioning system. For instance, it is particularly useful for SLAM and VIO, that were discussed in chapter 1. These enhancements would bring the UAVs closer to applications in search and rescue, inspection, and indoor navigation, where reliable attitude estimation is critical.

BIBLIOGRAPHY

[1] І. О. Довбиш, О. В. Муравйов, Р. М. Галаган, Г. А. Богдан, and А. С. Момот. Силові установки та джерела енергії сучасних БПЛА. *Вчені записки ТНУ імені В. І. Вернадського. Серія: Технічні науки*, 34(5): 16–21, 2023.

[2] О. В. Муравйов, І. О. Довбиш, Р. М. Галаган, Г. А. Богдан, and А. С. Момот. Перспективи розвитку технологій та підвищення рівня автономності БПЛА. *Вчені записки ТНУ імені В. І. Вернадського. Серія: Технічні науки*, 34(2):199–205, 2023.

[3] Review: Dji mini 4 pro drone. https://www.wired.com/review/dji-mini-4-drone/, . Accessed: 14.02.2025.

[4] https://nv.ua/ukr/ukraine/events/de-bayraktar-i-chi-efektivniy-bezpilotnik-u-2024-roci-proti-rosiyan-analiz-ekspertiv-50430579.html, . Accessed: 14.02.2025.

[5] Prodrone develops the “speed delivery”. https://www.prodrone.com/release-en/2874/, . Accessed: 14.02.2025.

[6] Ramy Rashad, Jelmer Goerres, Ronald Aarts, Johan B. C. Engelen, and Stefano Stramigioli. Fully actuated multirotor uavs: A literature review. *IEEE Robotics & Automation Magazine*, 27(3):97–107, 2020. doi: 10.1109/MRA.2019.2955964.

[7] Georgia Lykou, Dimitrios Moustakas, and Dimitris Gritzalis. Defending airports from uas: A survey on cyber-attacks and counter-drone sensing technologies. *Sensors*, 20:3537, 06 2020. doi: 10.3390/s20123537.

[8] Petryk V.F., Protasov A.G., Galagan R.M., Muraviov A.V., and Lysenko

I.I. Smartphone-based automated non-destructive testing devices. *Devices Methods Meas.*, 11:272–278, 2020.

[9] Муравьёв А. В. Основные тенденции, проблемы и перспективы развития дисплейной наноэлектроники. In *Неруйнівний контроль в контексті асоційованого членства України в Європейському союзі: матеріали 2-гої науково-технічної конференції з міжнародною участю*, pages 10–11, Польща, Люблін, 2018.

[10] Sameer Agrawal, Bhumeshwar K. Patle, and Sudarshan Sanap. Navigation control of unmanned aerial vehicles in dynamic collaborative indoor environment using probability fuzzy logic approach. *Cognitive Robotics*, 5: 86–113, 2025. ISSN 2667-2413. doi: https://doi.org/10.1016/j.cogr.2025.02.002.

[11] Khairul Nizam Tahar and Sarah Kamarudin. Uav onboard gps in positioning determination. *ISPRS - International Archives of the Photogrammetry, Remote Sensing and Spatial Information Sciences*, XLI-B1:1037–1042, 06 2016. doi: 10.5194/isprs-archives-XLI-B1-1037-2016.

[12] Young-Hwa Sung, Soo-Jae Park, Dong-Yeon Kim, and Sungho Kim. Gps spoofing detection method for small uavs using 1d convolution neural network. *Sensors*, 22(23), 2022. ISSN 1424-8220. doi: 10.3390/s22239412.

[13] Soulaimane Berkane and Abdelhamid Tayebi. Attitude and gyro bias estimation using gps and imu measurements. In *2017 IEEE 56th Annual Conference on Decision and Control (CDC)*, pages 2402–2407, 2017. doi: 10.1109/CDC.2017.8264001.

[14] Safar M. Asaad and Halgurd S Maghdid. A comprehensive review of indoor/outdoor localization solutions in iot era: Research challenges and fu-

ture perspectives. *Computer Networks*, 212:109041, 2022. ISSN 1389-1286. doi: https://doi.org/10.1016/j.comnet.2022.109041.

[15] Miaomiao Wang, Soulaimane Berkane, and Abdelhamid Tayebi. Nonlinear observers design for vision-aided inertial navigation systems. *IEEE Transactions on Automatic Control*, 67(4):1853–1868, 2022. doi: 10.1109/TAC.2021.3086459.

[16] Miaomiao Wang and Abdelhamid Tayebi. Nonlinear observers for stereo-vision-aided inertial navigation. 12 2019. doi: 10.1109/CDC40024.2019.9029563.

[17] Arnaud Taffanel, Barbara Rousselot, Jonas Danielsson, Kimberly Mcguire, Kristoffer Richardsson, Marcus Eliasson, Tobias Antonsson, and Wolfgang Hoenig. Lighthouse positioning system: Dataset, accuracy, and precision for uav research, 04 2021.

[18] Fuhu Che, Qasim Zeeshan Ahmed, Pavlos I. Lazaridis, Pradorn Sureephong, and Temitope Alade. Indoor positioning system (ips) using ultra-wide bandwidth (uwb)—for industrial internet of things (iiot). *Sensors*, 23 (12), 2023. ISSN 1424-8220. doi: 10.3390/s23125710.

[19] Balázs Nagy, Philipp Foehn, and Davide Scaramuzza. Faster than fast: Gpu-accelerated frontend for high-speed vio. In *2020 IEEE/RSJ International Conference on Intelligent Robots and Systems (IROS)*, pages 4361–4368, 2020. doi: 10.1109/IROS45743.2020.9340851.

[20] Giovanni Fusco and James M. Coughlan. Indoor localization using computer vision and visual-inertial odometry. In Klaus Miesenberger and Georgios Kouroupetroglou, editors, *Computers Helping People with Special Needs*, pages 86–93, Cham, 2018. Springer International Publishing. ISBN 978-3-319-94274-2.

[21] Anastasios I. Mourikis and Stergios I. Roumeliotis. A multi-state constraint kalman filter for vision-aided inertial navigation. In *Proceedings 2007 IEEE International Conference on Robotics and Automation*, pages 3565–3572, 2007. doi: 10.1109/ROBOT.2007.364024.

[22] Anton Kasyanov, Abi Baa, Jörg Stückler, and Bastian Leibe. Keyframe-based visual-inertial online slam with relocalization. 02 2017. doi: 10.48550/arXiv.1702.02175.

[23] Christian Forster, Matia Pizzoli, and Davide Scaramuzza. Svo: Fast semi-direct monocular visual odometry. In *2014 IEEE International Conference on Robotics and Automation (ICRA)*, pages 15–22, 2014. doi: 10.1109/ICRA.2014.6906584.

[24] Michael Bloesch, Sammy Omari, Marco Hutter, and Roland Siegwart. Robust visual inertial odometry using a direct ekf-based approach. In *2015 IEEE/RSJ International Conference on Intelligent Robots and Systems (IROS)*, pages 298–304, 2015. doi: 10.1109/IROS.2015.7353389.

[25] Dong Fu, Hao Xia, and Yanyou Qiao. Monocular visual-inertial navigation for dynamic environment. *Remote Sensing*, 13(9), 2021. ISSN 2072-4292. doi: 10.3390/rs13091610.

[26] Морозов М. А. and Муравьёв А. В. Современная лазерная дальнометрия. In *Новые направления развития приборостроения: материалы 9-й международной научнотехнической конференции молодых ученых и студентов*, page 38, Минск, Беларусь, 2016.

[27] E.A. Wan and R. Van Der Merwe. The unscented kalman filter for nonlinear estimation. In *Proceedings of the IEEE 2000 Adaptive Systems for Signal Processing, Communications, and Control Symposium*

(Cat. No.00EX373), pages 153–158, 2000. doi: 10.1109/ASSPCC.2000.882463.

[28] Sebastian O. H. Madgwick. An efficient orientation filter for inertial and inertial / magnetic sensor arrays. 2010.

[29] I. O. Dovbysh and O. V. Muraviov. Complementary filter for uav attitude estimation. In *Ефективність та автоматизація інженерних рішень у приладобудуванні: XX Всеукраїнська науково-практична конференція студентів, аспірантів та молодих вчених*, pages 295–298, Київ, 2024. КПІ ім. Ігоря Сікорського, ПБФ. 04–05 грудня 2024 р., Бібліогр.: 7 назв.

[30] Robert Mahony, T. Hamel, and Jean-Michel Pflimlin. Nonlinear complementary filters on the special orthogonal group. *Automatic Control, IEEE Transactions on*, 53:1203 – 1218, 07 2008. doi: 10.1109/TAC.2008.923738.

[31] Lucas Prado Osco, José Marcato Junior, Ana Paula Marques Ramos, Lúcio André de Castro Jorge, Sarah Narges Fatholahi, Jonathan de Andrade Silva, Edson Takashi Matsubara, Hemerson Pistori, Wesley Nunes Gonçalves, and Jonathan Li. A review on deep learning in uav remote sensing. *International Journal of Applied Earth Observation and Geoinformation*, 102:102456, 2021. ISSN 1569-8432. doi: https://doi.org/10.1016/j.jag.2021.102456.

[32] Andy Couturier and Moulay A. Akhloufi. A review on deep learning for uav absolute visual localization. *Drones*, 8(11), 2024. ISSN 2504-446X. doi: 10.3390/drones8110622.

[33] William Koch, Renato Mancuso, Richard West, and Azer Bestavros. Re-

inforcement learning for uav attitude control. *ACM Trans. Cyber-Phys. Syst.*, 3(2), February 2019. ISSN 2378-962X. doi: 10.1145/3301273.

[34] Stephen McGilvray Abdelhamid Tayebi. Attitude Stabilization of a VTOL Quadrotor Aircraft. *IEEE Transactions on Control Systems Technology*, 14 (3):562–571, 2006.

[35] Tolotra Samuel Randriakotonjanahary. *A low-cost, small scale Unmanned Aerial Vehicle capable of a real-time onboard deep learning-based object detection system*. PhD thesis, 11 2019.

[36] Куц Ю.В. *Новітні системи та технології: навчальний посібник* / Ю. В. Куц, Ю. Ю. Лисенко, А.С. Момот; КПІ ім. Ігоря Сікорського. – Київ: КПІ ім. Ігоря Сікорського, 2022. – 123 с.

[37] Stelmakh N., Mandrovska S. & Galagan R. Application of Resnet-152 neural networks to analyze images from UAV for fire detection. *Informatyka, Automatyka, Pomiary W Gospodarce I Ochronie Środowiska*. 2024. 14 (2). P. 77–82.

[38] Баженов В.Г. *Електроніка. Лабораторний практикум: навчальний посібник* / В. Г. Баженов, Є. Ф. Суслов, Ю. Ю. Лисенко, А.С. Момот; КПІ ім. Ігоря Сікорського. – Київ: КПІ ім. Ігоря Сікорського, 2022. – 70 с.